# Filling performance of Acid Blue 1 leveler on blind microvias

Mingjie Li [a], Xuesong Peng [a], Jie Jiang [a], Yaqiang Li [a, b, *], Fan Meng [a], Youzheng Wu [a], Maozhong An [a], Ruopeng Li [a, *], Penghui Ren [a, c, *], Peixia Yang [b, *]

[a] School of Chemistry and Chemical Engineering, Harbin Institute of Technology, Harbin 150001, China.

[b] College of Chemistry, Institute of Molecular Engineering Plus, Fuzhou University, Fuzhou 350116, Fujian, China

[c] Shandong Laboratory of Advanced Materials and Green Manufacturing at Yantai, Yantai 264000, P. R. China.

* Corresponding authors

E-mail: liyaqiang@fzu.edu.cn, liruopeng630@163.com, phren132@126.com, yangpeixia@hit.edu.cn

Cyclic voltammetry (CV) is a widely-accepted method to study additives. It is often used to calculate the anodic stripping coulomb (ASC) in CV curves to analyze effects of additives quantitively. As for ASC calculation, the x-axis of potential can be transformed into time (s). By integrating anodic area can solve ASC. The integration equal is shown as follows:

$$Q = \int i\mathrm{d}t \qquad \text{Eq. S1}$$

Where $Q$ is anodic stripping coulomb, $i$ represents current density (A/dm$^2$), $t$ is time (s).

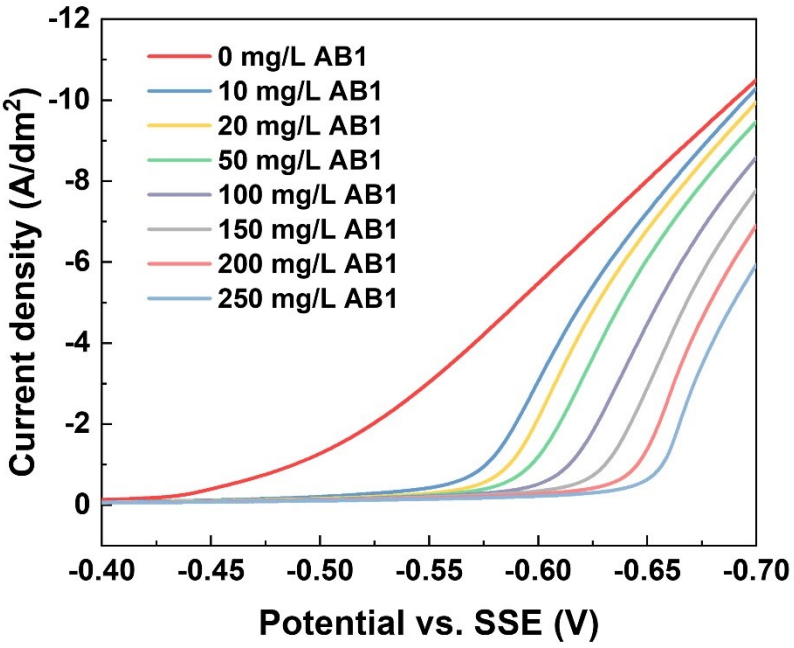


**Fig. S1** Cathodic sweeping curves in Cyclic voltammetry with different AB1 concentration measured with 50 mV/s and 1000 rpm.

Fig. S1 shows that the cathodic onset potential shifts negatively with AB1 rising from 0 mg/L to 250 mg/L, indicating that AB1 is of suppressing effect and its suppressing is strengthened continuously.

Fig. S2 shows the molecular formula of AB1 and optimized AB1 structure, respectively.

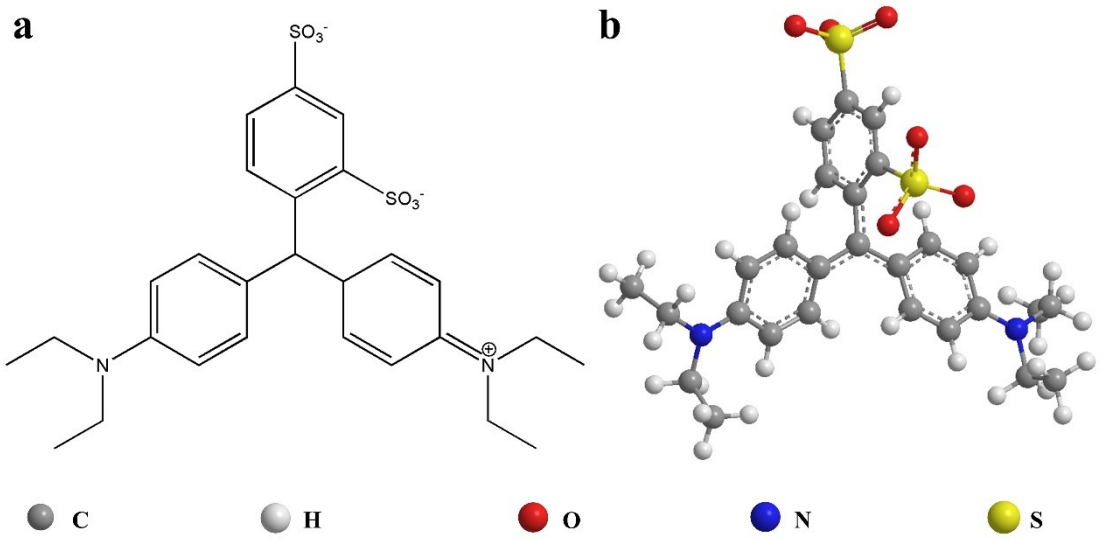


**Fig. S2** (a) Molecular formula of AB1 and (b) optimized AB1 molecular structure.

Fig. S3 shows the top view of adsorption configuration. Brown color means carbon atom, pastel grey means hydrogen atom, red color means oxygen atom, bluish grey means nitrogen atom, yellow color means sulfur atom. Besides, blue color means the depletion of charge and yellow color indicates the accumulation of charge. The charge transfer between -$SO_3$ functional group of AB1 and copper substrate indicates that there is obvious adsorption interaction between AB1 and copper substrate.

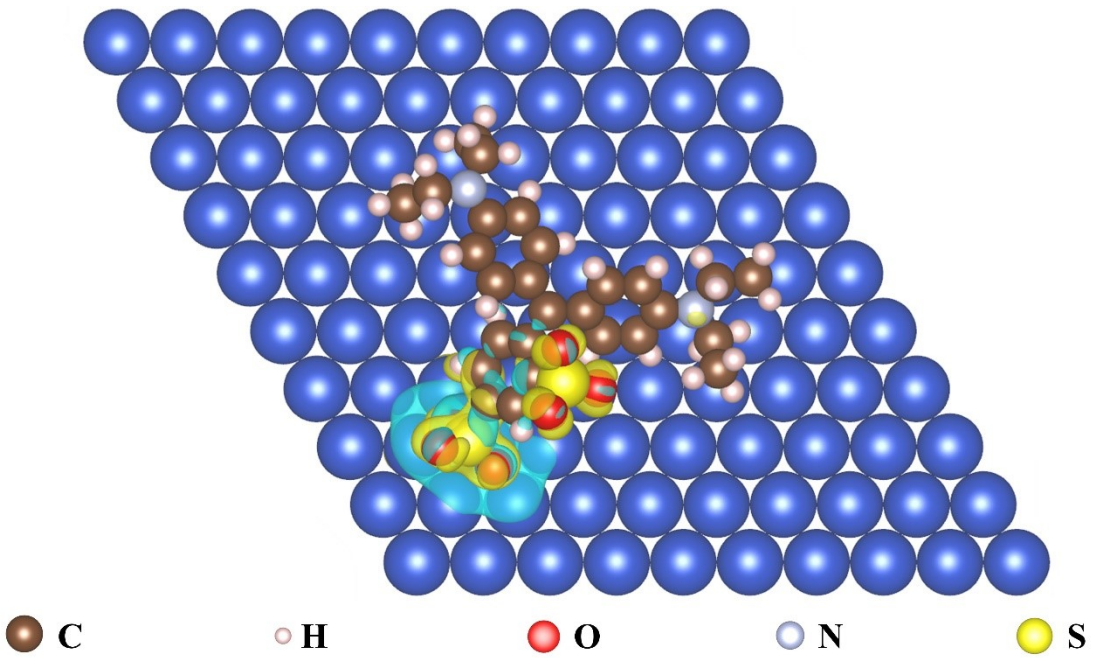


**Fig. S3** Top view of adsorption equilibrium configuration.

Tab. S1 shows the band assignments for AB1 during in situ infrared spectroscopy. The characteristic peaks at 1080 $cm^{-1}$ and 1220 $cm^{-1}$ attribute to stretching vibration of

-$SO_3$ functional group. 1630 $cm^{-1}$ is the stretching vibration of C-N, while 1420 $cm^{-1}$ and 3223 $cm^{-1}$ attribute to C-C and C-H stretching vibration of aromatic ring, respectively.

**Tab. S1** IR characteristic band assignments for Acid Blue 1.

| Band position/$cm^{-1}$ | Band assignment | Ref |
|---|---|---|
| 1080 | ν (-$SO_3$) | [1] |
| 1220 | ν (-$SO_3$) | [1] |
| 1420 | ν (aromatic C-C) | [2] |
| 1630 | ν (C-N) | [3] |
| 3223 | ν (aromatic C-H) | [4] |

ν: stretching modes

Fig. S4 shows the top view of microvias after electroplating. The surface is flat and compact without any holes or uneven bump, indicating that the obtained copper layer is of low roughness, beneficial for lowering the signal losses during high frequency transmission.

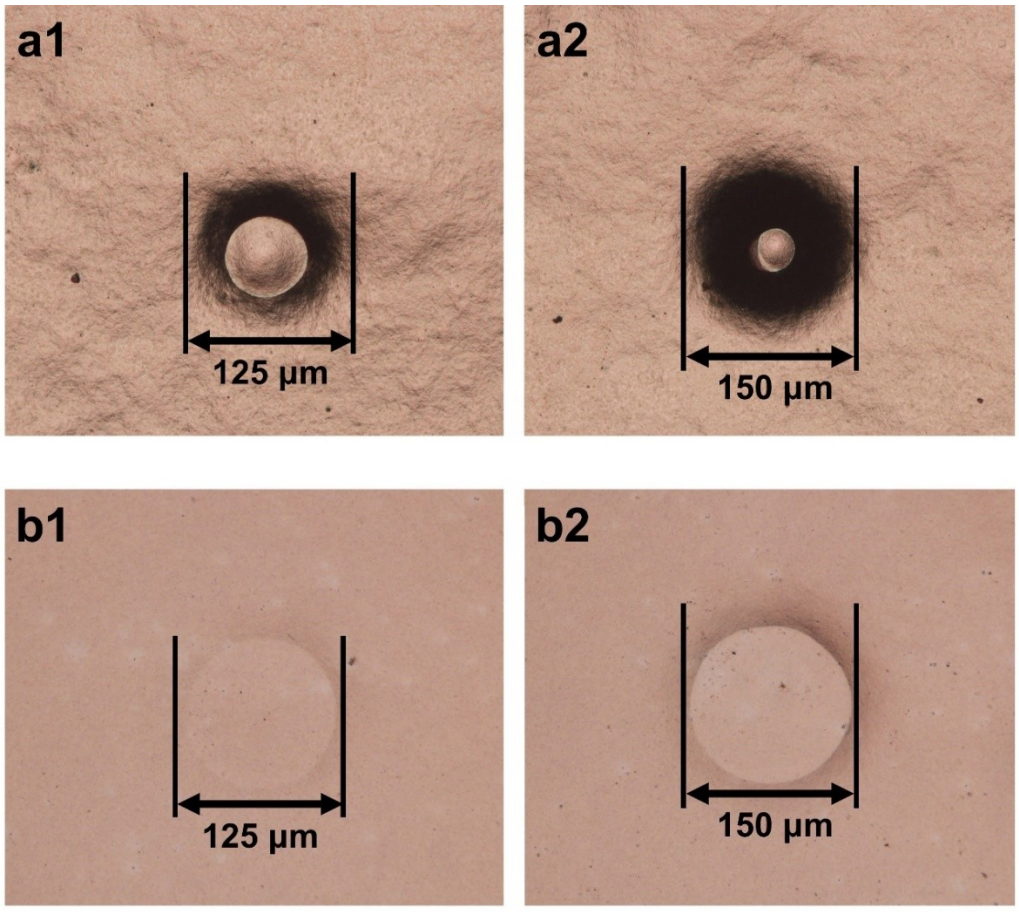


**Fig. S4** Top view of copper layer for filling microvias with different diameters obtained with (a) 0 mg/L AB1 and (b) 20 mg/L AB1.

Fig. S5 shows the filling performance of most-used leveler Janus Green B (JGB). Although void-free filling is achieved in microvias with diameters of 125 μm and 150 μm, the copper layer morphology is full of small gas holes from top view. In contrast to copper layer obtained with AB1, the roughness $R_z$ is 298 nm (Fig. S4c), indicating that the signal loss of copper layer obtained with JGB is larger than that with AB1. Laterally, the signal losses during high frequency transmission for copper layer obtained with JGB was simulated, as shown in figure S4d. By comparison with Fig. 5c, the signal loss for copper layer obtained with JGB is larger than that obtained with JGB

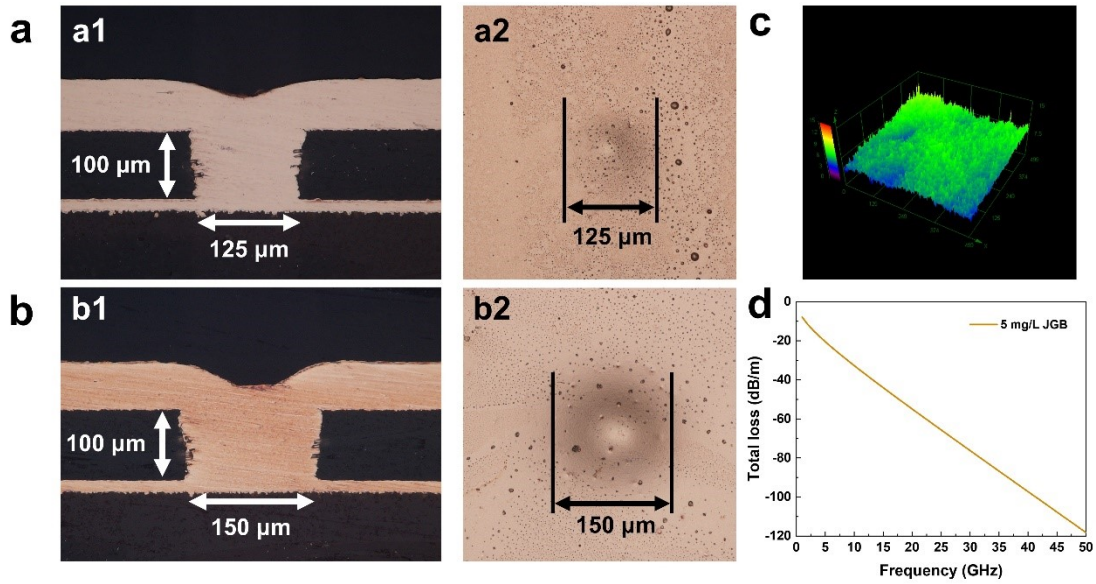


at the same transmission frequency.

**Fig. S5** (a) Cross-sectional figure (a1) and top figure (a2) with diameter of 125 μm. (b) Cross-sectional figure (b1) and top figure (b2) with diameter of 150 μm. (c) Surface roughness of copper layer obtained with JGB. (d) Simulated signal loss for copper layer obtained with JGB. Electroplating process: 250 g/L $CuSO_4 \cdot 5H_2O$, 40 g/L $H_2SO_4$, 60 mg/L $Cl^-$, 2 mg/L SPS, 200 mg/L PEG and 5 mg/L JGB, 3 A/dm$^2$ for 3h.

Fig. S6 shows the cyclic voltammetry measured without $Cu^{2+}$. It can be seen that the curve obtained with 20 mg/L AB1 almost overlaps with that of 0 mg/L AB1. And there is no cathodic electroreduction reaction peak appeared, which illustrates that there is no decomposition reaction occurred in AB1 during electroplating and AB1 is of good stability in electroplating solution.

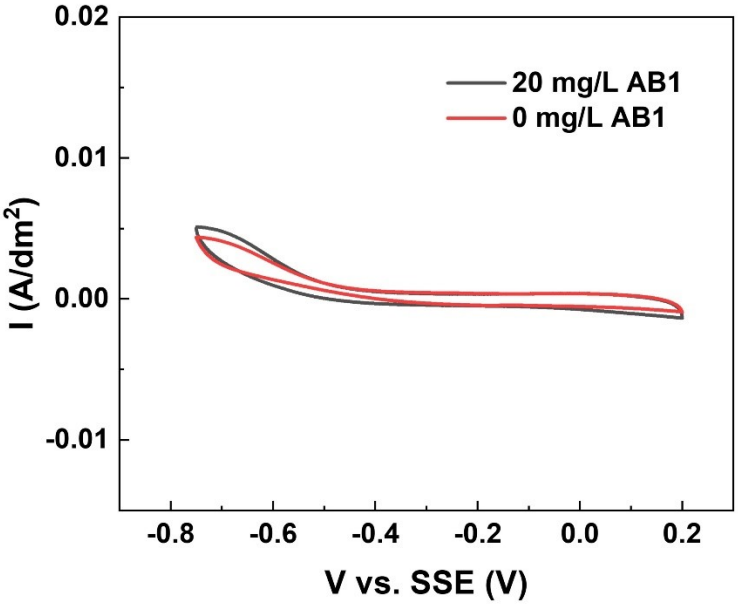


**Fig. S6** Cyclic voltammetry curve obtained without $Cu^{2+}$. The scanning rate and rotating speed is 50 mV/s and 1000 rpm.

Fig. S7 shows the electroplating results from electroplating solution with different coulomb introduced. No defects formed further indicate that AB1 is of good stability in electroplating solution and during electroplating process.

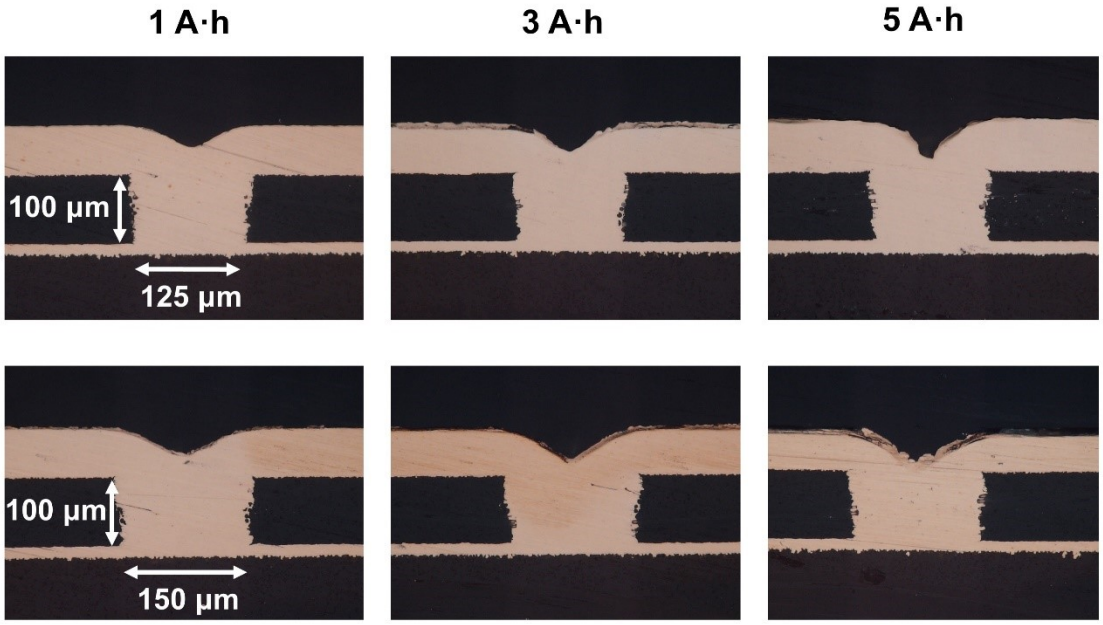


**Fig. S7** Top view of copper layer for filling microvias with diameters of (a) 125 μm and (b) 150 μm. AB1 concentration was 20 mg/L.

Molecular dynamics (MD) simulation is an effective method to obtain the diffusion coefficient of additives. In this work, Material Studio was accepted to

simulate the dynamics of AB1. The simulation box was 2.56 nm× 2.56 nm× 2.56 nm. There were 1 AB1 molecule and water molecules of 1 g $cm^{-3}$ in the simulation box. During MD simulation, COMPASS (Condensed-Phase Optimized Molecular Potentials for Atomistic Simulation Studies) force field and NVT ensemble was applied [5], while the temperature and simulation time was 298K and 300 ps with time step of 1fs. Diffusion coefficient of AB1 was solved based on Einstein equation as follows:

$$D = \frac{1}{6t}\left[\left|r_A(t) - r_A(0)\right|^2\right] = \frac{1}{6t}MSD \quad \text{Eq. S2}$$

Where D was diffusion coefficient, $r_A(t)$ and $r_A(0)$ was position of additive on t time and t=0, respectively, t was simulation time. The simulated results were shown in Fig. S8. Diffusion coefficient for AB1 ($D_{AB1}$) was $2\times10^{-10}$ $m^2$ $s^{-1}$, the same order as $D_{PEG}$ ($1\times10^{-10}$ $m^2$ $s^{-1}$) [6] and one order smaller than that of SPS ($5\times10^{-9}$ $m^2$ $s^{-1}$) [7], which demonstrates that the diffusion transport supplying rate of AB1 and PEG is far smaller than supplying rate of SPS within microvias during electroplating, meaning that the ratio of SPS to AB1 is increased within microvias. However, the transport of AB1 and PEG is not limited on the opening area owing to convection, indicating that the ratio of SPS to AB1 is smaller than that at the bottom of microvias. As a result, effective growth rate difference is formed within microvias and copper grows from bottom to top.

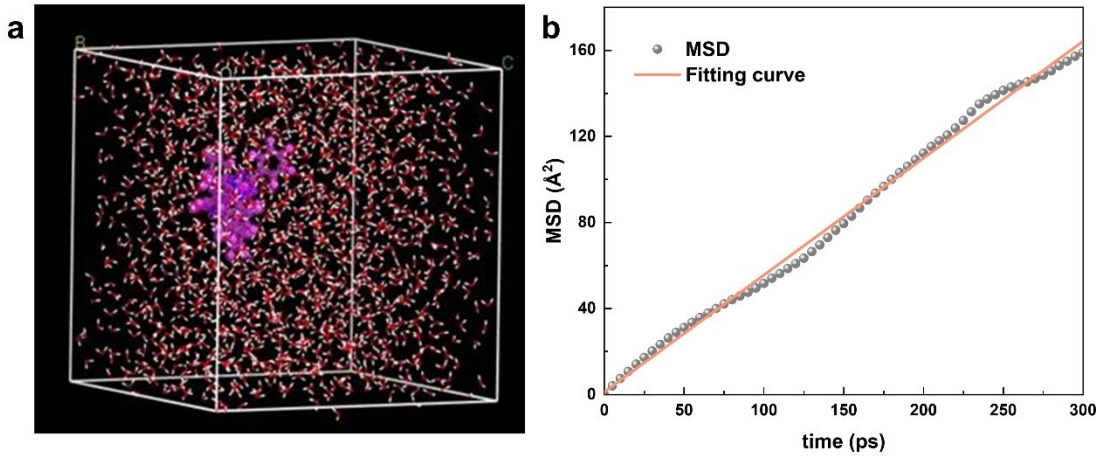


**Fig. S8** (a) Molecular dynamics simulation of AB1 and (b) simulated MSD-t curve.

## Reference

[1] Weng Shipu, Xu Yizhuang. Fourier Transform Infrared Spectroscopy Analysis. Beijing: Chemical Industry Press, 2016.

[2] Sarika H. V., Ravin M. J. Adsorptive removal of crystal violet from aqueous

solution by cross-linked chitosan coated bentonite. Materials Today: Proceedings, 2020, 29: 1025-1032.

[3] Fenghong L., Ansgar W., Martin P., et al. Leuco Crystal Violet as a Dopant for n-Doping of Organic Thin Films of Fullerene C60. Journal of Physical Chemistry B, 2004, 108: 17076-17082.

[4] Hassan A., Mostafa H. B., Reyhaneh K., et al. One-step hydrothermally synthesized ferrite@polymeric nanoparticles for decolorization of crystal violet. Desalination and Water Treatment, 2018, 108: 299-310.

[5] Xu W., Shengtao Z., Shijin C., et al. Effects of 2,2-Dithiodipyridine as a Leveler for Through-Holes Filling by Copper Electroplating. Journal of The Electrochemical Society, 2019, 166 (13): D660-D668.

[6] Yuwen H. H., Zhang X. P. Numerical simulation of the TSV-Cu filling by electroplating process with the accelerator and suppressor. 17th International Conference on Electronic Packaging Technology, 2016: 721-726.

[7] Childers A. S., Johnson M. T., Ramirez-Rico J., et al. Modeling Macro-Sized, High Aspect Ratio Through-Hole Filling by Multi-Component Additive-Assisted Copper Electrodeposition. Journal of The Electrochemical Society, 2013, 160 (12): D3093-D3102.